

Analysis of the Dynamics of a Predator-prey Model with Holling Functional Response

Hongyu Chen¹ and Chunrui Zhang^{1,†}

Abstract A diffusive predator-prey system with Holling functional response is considered. Firstly, existence of positive equilibrium of this reaction diffusion model under Neumann boundary condition is obtained. Meanwhile, the existence conditions for Turing instability and Hopf bifurcations of a system with Holling II functional response are established. Next, the existence of the hydra effect is demonstrated, when the system is undergoing non-homogeneous steady-state solutions. Finally, numerical simulations are illustrated to support our theory results.

Keywords Predator-prey model, Turing instability, Hopf bifurcation, Hydra effect.

MSC(2010) 34C23, 35K57.

1. Introduction

Dynamics of predator-prey model is one of important subjects in mathematical ecology, and some important results have been studied and derived by many researchers [8, 10, 15, 18, 19, 21–23]. The earliest population can be traced back to 1798, the Malthus model proposed by T. R. Malthus. In 1838, the Dutch biologist P. Verhulst introduced the largest population that the natural environment could withstand on the basis of this model, and proposed the famous Logistic model. In 1948, P. H. Leslie and J. C. Gower extended the Logistic model, and proposed the Leslie-Gower system model. With the development, people gradually discovered that the functional response function should not be a simple linear function, and a more reasonable functional response function should be nonlinear and bounded. C. S. Holling proposed three bounded functional response functions [4, 6, 7, 9, 13, 24]. The results of the above population research include stability, the existence of limit cycles, bifurcation and other issues [5, 11, 14, 20].

The hydra effect is a phenomenon in which population balance or time average density increases when the mortality rate of the population increases [1, 2]. In [1], the three key mechanisms underlying the hydra effect were proposed by Abrams. The two latter mechanisms were investigated in [12]. However, this mechanism has been determined in the theoretical research conducted by [16], in which they analyzed predator-prey models with Holling II and III functional responses. Regarding the hydra effect, the paper by Strevens and Bonsall [17] discussed harvesting strategies

[†]the corresponding author.

Email address: math@nefu.edu.cn (C. Zhang), 2776488694@qq.com (H. Chen)

¹School of Science, Northeast Forestry University, Harbin, Heilongjiang 150040, China

in a host-parasitic wasp complex population system. In [3], a diffusive predator-prey model with functional response function was studied

$$\begin{cases} \frac{\partial R}{\partial t} = D_R \frac{\partial^2 R}{\partial x^2} + rR(1 - \frac{R}{K}) - F(R)C, \\ \frac{\partial C}{\partial t} = D_C \frac{\partial^2 C}{\partial x^2} + ef_{RC}F(R)C - m_C C - q_C C^2, \end{cases} \quad (1.1)$$

where

$$F(R) = \frac{a_{CR}R^n}{1 + a_{CR}Th_{CR}R^n}. \quad (1.2)$$

The authors have shown the occurrence of the hydra effect in some of its steady-state dynamics through numerical simulations. Substituting equation (1.2) into system (1.1), system (1.3) can be obtained. In this paper, we will analyze the dynamic properties of the model (1.3). The system is as follows:

$$\begin{cases} \frac{\partial R}{\partial t} = D_R \frac{\partial^2 R}{\partial x^2} + rR(1 - \frac{R}{K}) - \frac{a_{CR}R^n C}{1 + a_{CR}Th_{CR}R^n}, \\ \frac{\partial C}{\partial t} = D_C \frac{\partial^2 C}{\partial x^2} + \frac{ef_{RC}a_{CR}R^n C}{1 + a_{CR}Th_{CR}R^n} - m_C C - q_C C^2, \end{cases} \quad (1.3)$$

and the Neumann boundary condition

$$\begin{aligned} R_x(x, t) = C_x(x, t) = 0, R_x(l, t) = C_x(l, t) = 0, t > 0, \\ R(x, 0) = R_0(x) \geq 0, C(x, 0) = C_0(x) \geq 0, x \in [0, l], \end{aligned} \quad (1.4)$$

where R and C are the density of the prey and the density of the predator respectively, and r is the inherent growth rate of the prey R . K is the environmental capacity of the prey R . m_C is the per capita mortality of the species C that is not related to density, and q_C is per capita mortality of species C related to density. D_R and D_C are the diffusion coefficients of species R and C respectively, and ef_{RC} is the conversion coefficient from species R to species C . a_{CR} is the attack coefficient of species C against species R , and Th_{CR} is the effect time of species C on species R . All parameters are strictly positive constants.

In this paper, we analyze the Turing instability and the existence of Hopf bifurcations of the system (1.3), when $n = 1$. The existence of the hydra effect is shown, when the system (1.3) is undergoing the state bifurcation. The structure of this article is arranged as follows: In Section 2, by analyzing the characteristic equation of the coexistence balance system, we clarify conditions for the existence of Turing unstable and Hopf bifurcations of a diffusive predator-prey system. In addition, we also determine the critical Turing bifurcation and Turing instability curves in the parameter plane. Then, numerical simulations are explained to support the existence of the hydra effect and other theoretical analysis results in Section 3. Finally, in Section 4, we discuss and conclude.

2. Turing instability and Hopf bifurcation analysis

2.1. Existence of positive equilibrium

In this section, we discuss the existence of the positive equilibrium point of system (1.1). In the system (1.1), we set

$$\begin{cases} f(R, C) = rR(1 - \frac{R}{K}) - F(R)C = 0, \\ g(R, C) = ef_{RC}F(R)C - m_C C - q_C C^2 = 0. \end{cases} \quad (2.1)$$

From the second equation of (2.1), we can get

$$C = \frac{ef_{RC}F(R) - m_C}{q_C}. \tag{2.2}$$

Substituting C into the first equation of (2.1) with formula (2.2), we obtain equation about $F(R)$

$$\frac{ef_{RC}}{q_C}F^2(R) - \frac{m_C}{q_C}F(R) - rR(1 - \frac{R}{K}) = 0.$$

Denote

$$Y(R) = \frac{ef_{RC}}{q_C}F^2(R) - \frac{m_C}{q_C}F(R) - rR(1 - \frac{R}{K}),$$

we can find $Y(0) = -r < 0$ and $Y(+\infty) > 0$, when $R > 0$. Therefore, there is at least one positive solution R_* , which meets $Y(R_*) = 0$. Using (2.2), we can get $C_* = \frac{ef_{RC}F(R_*) - m_C}{q_C}$. Set $C_* > 0$, then the system (1.1) has at least one positive equilibrium (R_*, C_*) . Through the above analysis, we can get the following theorem.

Theorem 2.1. *Assuming $R_* > 0$, if $ef_{RC}a_{CR}R_*^n - m_C(1 + a_{CR}Th_{CR}R_*^n) > 0$, the system (1.1) has a positive equilibrium point (R_*, C_*) .*

In the following, we use a graphical method to illustrate the existence of a positive equilibrium point. Denote

$$Y_1(R) = \frac{ef_{RC}a_{CR}^2R^{2n}}{q_C(1 + a_{CR}Th_{CR}R^n)^2} - \frac{m_Ca_{CR}R^n}{q_C(1 + a_{CR}Th_{CR}R^n)},$$

$$Y_2(R) = rR(1 - \frac{R}{K}),$$

when n takes the value 1, 2, 3, 4, we draw four graphs of $Y_1(R)$ and $Y_2(R)$, as shown in Figure 1. Obviously, R_* is the intersection of $Y_1(R)$ and $Y_2(R)$.

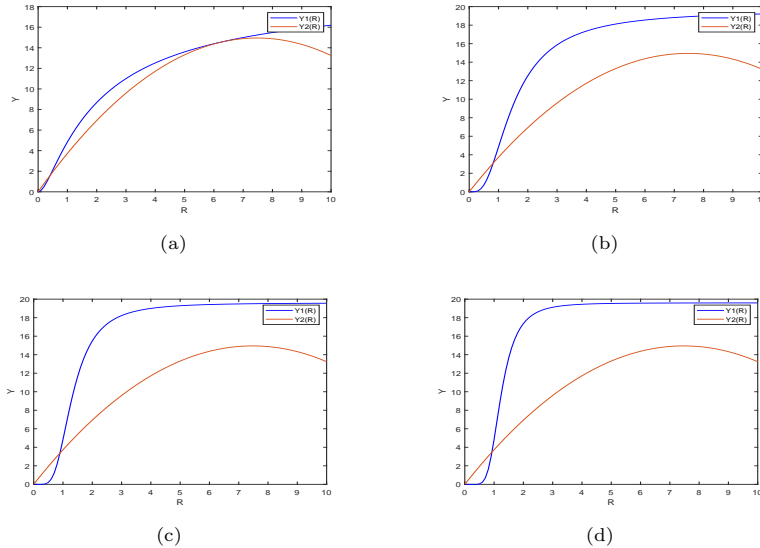


Figure 1. (a), (b), (c), (d) describe the figures of functions $Y_1(R)$ and $Y_2(R)$ in (R, Y) plane, when n takes 1, 2, 3, 4, respectively. Keeping the other parameters fixed at the values: $r = 4, m_C = 0.0201, K = 14.95, a_{CR} = 1.01, Th_{CR} = 1, ef_{RC} = 1, q_C = 0.05$.

2.2. Linear stability analysis

In this section, we conduct a linear stability analysis of system (1.3). In order to simplify the discussion of system (1.3), we transform positive equilibrium point (R_*, C_*) into $(0, 0)$ by the means of transformation $(R, C) = (R_* + \tilde{R}, C_* + \tilde{C})$. Then, we can obtain the linearized system structure as follows:

$$\begin{cases} \frac{\partial \tilde{R}}{\partial t} = D_R \frac{\partial^2 \tilde{R}}{\partial x^2} + [r(1 - \frac{2R_*}{K}) - \frac{na_{CR}R_*^{n-1}C_*}{(1+a_{CR}Th_{CR}R_*^n)^2}] \tilde{R} - \frac{a_{CR}R_*^n}{1+a_{CR}Th_{CR}R_*^n} \tilde{C}, \\ \frac{\partial \tilde{C}}{\partial t} = D_C \frac{\partial^2 \tilde{C}}{\partial x^2} + \frac{a_{CR}ef_{RC}nR_*^{n-1}C_*}{(1+a_{CR}Th_{CR}R_*^n)^2} \tilde{R} + (-m_C - 2q_C C_* + \frac{a_{CR}ef_{RC}R_*^n}{1+a_{CR}Th_{CR}R_*^n}) \tilde{C}. \end{cases} \tag{2.3}$$

Denote

$$\begin{aligned} p_1 &= r(1 - \frac{2R_*}{K}) - \frac{na_{CR}R_*^{n-1}C_*}{(1+a_{CR}Th_{CR}R_*^n)^2}, \\ p_2 &= -m_C - 2q_C C_* + \frac{a_{CR}ef_{RC}R_*^n}{1+a_{CR}Th_{CR}R_*^n}, \\ q_1 &= \frac{a_{CR}R_*^n}{1+a_{CR}Th_{CR}R_*^n}, \\ q_2 &= \frac{a_{CR}ef_{RC}nR_*^{n-1}C_*}{(1+a_{CR}Th_{CR}R_*^n)^2}. \end{aligned}$$

Let $D_R = \varepsilon d$, $D_C = d$, then we can get $\varepsilon = \frac{D_R}{D_C} > 0$. Rewrite equation (2.3) as follows:

$$\begin{cases} \frac{\partial \tilde{R}}{\partial t} = \varepsilon d \frac{\partial^2 \tilde{R}}{\partial x^2} + p_1 \tilde{R} - q_1 \tilde{C}, \\ \frac{\partial \tilde{C}}{\partial t} = d \frac{\partial^2 \tilde{C}}{\partial x^2} + q_2 \tilde{R} + p_2 \tilde{C}. \end{cases} \tag{2.4}$$

We can obtain Jacobian matrix

$$A = \begin{pmatrix} -\varepsilon d u_k + p_1 & -q_1 \\ q_2 & -d u_k + p_2 \end{pmatrix},$$

where $u_k = \frac{k^2 \pi^2}{l^2}$. Then, the characteristic equation of A is as follows:

$$D_k(\lambda, \varepsilon) = \lambda^2 - TR_k \lambda + DET_k = 0$$

with

$$\begin{aligned} TR_k &= -(\varepsilon + 1) \frac{dk^2 \pi^2}{l^2} + p_1 + p_2, \\ DET_k &= \varepsilon \frac{d^2 k^4 \pi^4}{l^4} - (p_1 + p_2 \varepsilon) \frac{dk^2 \pi^2}{l^2} + p_1 p_2 + q_1 q_2. \end{aligned}$$

We assume that

$$(B_0) \begin{cases} p_1 + p_2 < 0, \\ p_1 p_2 + q_1 q_2 > 0. \end{cases}$$

Lemma 2.1. *Suppose that (B_0) holds, then the ordinary differential equation system corresponding to the system (1.3) is locally asymptotically stable at the positive equilibrium point (R_*, C_*) .*

Proof. We can get the characteristic equation of ordinary differential equation system, when the diffusion term is not added. That is,

$$D_0(\lambda, \varepsilon) = \lambda^2 - TR_0\lambda + DET_0 = 0$$

with

$$\begin{aligned} TR_0 &= p_1 + p_2, \\ DET_0 &= p_1p_2 + q_1q_2. \end{aligned}$$

Both roots of $D_0(\lambda, \varepsilon) = 0$ have negative real parts, when $TR_0 < 0$ and $DET_0 > 0$. Therefore, the system (1.3) is asymptotically stable at the positive equilibrium point (R_*, C_*) . Hence, the lemma is proved. \square

2.3. Analysis of Turing instability

In this section, we mainly study the existence condition of Turing instability at the positive equilibrium point (R_*, C_*) of system (2.5) with Holling II functional response, which is system (1.3), when $n = 1$.

$$\begin{cases} \frac{\partial R}{\partial t} = \varepsilon d \frac{\partial^2 R}{\partial x^2} + rR(1 - \frac{R}{K}) - \frac{a_{CR}RC}{1+a_{CR}Th_{CR}R}, \\ \frac{\partial C}{\partial t} = d \frac{\partial^2 C}{\partial x^2} + \frac{ef_{RC}a_{CR}RC}{1+a_{CR}Th_{CR}R} - m_C C - q_C C^2. \end{cases} \quad (2.5)$$

According to Theorem 2.1, we can get that when $ef_{RC}a_{CR}R_* - m_C(1+a_{CR}Th_{CR}R_*) > 0$, the system (2.5) has a positive equilibrium point (R_*, C_*) . Further, according to the above method, we can get the characteristic equation of system (2.5), which is the result of Section 2.2

$$D_k(\lambda, \varepsilon) = \lambda^2 - TR_k\lambda + DET_k = 0 \quad (2.6)$$

with

$$\begin{aligned} TR_k &= -(\varepsilon + 1) \frac{dk^2\pi^2}{l^2} + p'_1 + p'_2, \\ DET_k &= \varepsilon \frac{d^2k^4\pi^4}{l^4} - (p'_1 + p'_2\varepsilon) \frac{dk^2\pi^2}{l^2} + p'_1p'_2 + q'_1q'_2, \end{aligned}$$

where

$$\begin{aligned} p'_1 &= r(1 - \frac{2R_*}{K}) - \frac{a_{CR}C_*}{(1 + a_{CR}Th_{CR}R_*)^2}, \\ p'_2 &= -m_C - 2q_C C_* + \frac{a_{CR}ef_{RC}R_*}{1 + a_{CR}Th_{CR}R_*}, \\ q'_1 &= \frac{a_{CR}R_*}{1 + a_{CR}Th_{CR}R_*}, \\ q'_2 &= \frac{a_{CR}ef_{RC}C_*}{(1 + a_{CR}Th_{CR}R_*)^2}. \end{aligned}$$

At this point, (B_0) still holds. For the convenience of notation, all p_1, p_2, q_1, q_2 mentioned below refers to p'_1, p'_2, q'_1, q'_2 .

Now, we consider the existence conditions for Turing instability.

Assume that

$$(B_1) \quad 0 < \varepsilon < \varepsilon_1, \varepsilon_1 = \frac{p_1 p_2 + 2q_1 q_2}{p_2^2} - 2\sqrt{\frac{p_1 p_2 q_1 q_2 + q_1^2 q_2^2}{p_2^4}}.$$

$$(B_2) \quad 0 < \varepsilon < \varepsilon_2(d), \varepsilon_2(d) = \frac{p_1 l^2}{d\pi^2 - p_2 l^2}.$$

$\varepsilon = \varepsilon_2(d)$ decreases monotonically in d and intersects with $\varepsilon = \varepsilon_1$ at the point $d = d_0$. We take $\varepsilon_B(d) = \min_{d>0} \{\varepsilon_1, \varepsilon_2(d)\}$, then

$$\varepsilon_B(d) = \begin{cases} \varepsilon_1, & 0 < d \leq d_0, \\ \varepsilon_2(d), & d > d_0. \end{cases} \quad (2.7)$$

Hence, we have the following lemma.

Lemma 2.2. *Suppose that (B_0) holds, then assumptions (B_1) and (B_2) hold, if and only if $0 < \varepsilon < \varepsilon_B(d)$, $d > 0$.*

Proof. Let $x = \frac{dk^2\pi^2}{l^2} > 0$, then we rewrite DET_k as

$$DET_k = \varepsilon x^2 - (p_1 + p_2 \varepsilon)x + p_1 p_2 + q_1 q_2.$$

Then, we can get symmetry axis is $x = \frac{p_1 + p_2 \varepsilon}{2\varepsilon}$, and at this time, DET_k can be taken to a minimum. That is,

$$DET_{kmin} = p_1 p_2 + q_1 q_2 - \frac{(p_1 + p_2 \varepsilon)^2}{4\varepsilon}.$$

Since $x > 0$, we have $p_1 + p_2 \varepsilon > 0$. If we want $DET_{kmin} < 0$ with the condition $p_1 + p_2 \varepsilon > 0$, ε must satisfy $p_1 p_2 + q_1 q_2 - \frac{(p_1 + p_2 \varepsilon)^2}{4\varepsilon} < 0$. We can obtain

$$0 < \varepsilon < \frac{p_1 p_2 + 2q_1 q_2}{p_2^2} - 2\sqrt{\frac{p_1 p_2 q_1 q_2 + q_1^2 q_2^2}{p_2^4}},$$

when

$$p_1 > 0, p_2 < -p_1, q_1 > 0, q_2 > -\frac{p_1 p_2}{q_1}.$$

Let $\varepsilon_1 = \frac{p_1 p_2 + 2q_1 q_2}{p_2^2} - 2\sqrt{\frac{p_1 p_2 q_1 q_2 + q_1^2 q_2^2}{p_2^4}}$, then when $0 < \varepsilon < \varepsilon_1$, it can be ensured that the symmetry axis is greater than 0, and Turing instability will occur at (R_*, C_*) .

Then, we take x between the symmetry axis and the right root of $DET_k = 0$. That is, $\frac{p_1 + p_2 \varepsilon}{2\varepsilon} \leq x \leq \frac{p_1 + p_2 \varepsilon + \sqrt{\Delta}}{2\varepsilon}$. When x takes a value on the axis of symmetry, k can be taken to the minimum, and we can get

$$k_{min}^2 = \frac{p_1 + p_2 \varepsilon}{2\varepsilon} \cdot \frac{l^2}{d\pi^2},$$

$$k_{min} = \sqrt{\frac{p_1 + p_2 \varepsilon}{2\varepsilon} \cdot \frac{l^2}{d\pi^2}}.$$

By making sure $\sqrt{\frac{1}{2} \cdot \frac{p_1 + p_2 \varepsilon}{\varepsilon} \cdot \frac{l^2}{d\pi^2}} > \sqrt{\frac{1}{2}}$, we can obtain

$$0 < \varepsilon < \frac{p_1 l^2}{d\pi^2 - p_2 l^2},$$

when

$$d > 0, p_1 > 0, p_2 < -p_1, q_1 > 0, q_2 > -\frac{p_1 p_2}{q_1}.$$

Let $\varepsilon_2(d) = \frac{p_1 l^2}{d\pi^2 - p_2 l^2}$, we can find that $\varepsilon = \varepsilon_2(d)$ decreases monotonically in d and intersects with $\varepsilon = \varepsilon_1$ at the point $d = d_0$, where

$$d_0 = \frac{2(-p_1 p_2^2 l^2 - p_2 q_1 q_2 l^2 + p_2^3 \sqrt{\frac{q_1 q_2 (p_1 p_2 + q_1 q_2)}{p_2^4}} l^4)}{\pi^2(-p_1 p_2 - 2q_1 q_2 + 2p_2^2 \sqrt{\frac{q_1 q_2 (p_1 p_2 + q_1 q_2)}{p_2^4}})}.$$

□

Next, the boundary of Turing's instability is determined.

Denote

$$\varepsilon_*(k, d) = \frac{l^2 [p_1 d k^2 \pi^2 - p_1 p_2 l^2 - q_1 q_2 l^2]}{d k^2 \pi^2 (d k^2 \pi^2 - p_2 l^2)}, d > d_k, \quad (2.8)$$

where $d_k = \frac{p_1 p_2 l^2 + q_1 q_2 l^2}{p_1 k^2 \pi^2}$.

Then, $DET_k = 0$, when $\varepsilon = \varepsilon_*(k, d)$.

That is,

$$DET_k = 0 \Leftrightarrow \varepsilon_*(k, d) = \frac{l^2 [p_1 d k^2 \pi^2 - p_1 p_2 l^2 - q_1 q_2 l^2]}{d k^2 \pi^2 (d k^2 \pi^2 - p_2 l^2)}.$$

Then,

$$\frac{d\varepsilon_*}{dx} = \frac{-p_1 x^2 + 2p_1 p_2 x + 2q_1 q_2 x - p_2 q_1 q_2 - p_1 p_2^2}{x^2 (x - p_2)^2},$$

and we can get

$$d = \frac{p_1 p_2 + q_1 q_2 + \sqrt{p_1 p_2 q_1 q_2 + q_1^2 q_2^2}}{p_1} \cdot \frac{l^2}{k^2 \pi^2}.$$

Set $d_M = \frac{p_1 p_2 + q_1 q_2 + \sqrt{p_1 p_2 q_1 q_2 + q_1^2 q_2^2}}{p_1} \cdot \frac{l^2}{k^2 \pi^2}$, then $\frac{d\varepsilon_*}{dx} = 0$, when $d = d_M$. At this time, $\varepsilon_*(k, d)$ reaches the maximum value ε_1 .

Lemma 2.3. *Suppose that (B_0) holds, function $\varepsilon = \varepsilon_*(k, d)$ has the following properties:*

- (1) *When $0 < d < d_M(k)$, $\varepsilon_*(k, d)$ increases monotonously, and when $d > d_M(k)$, $\varepsilon_*(k, d)$ decreases monotonously.*
- (2) *As for $k_i < k_{i+1}$, $k_i \in N$, $i = 1, 2, 3, \dots$, there is only one root $d_{k_1, k_2} \in (d_M(k_2), d_M(k_1))$ satisfies $\varepsilon_*(k_1, d) = \varepsilon_*(k_2, d)$ for $d > 0$. Furthermore,*

$$\varepsilon_*(k_1, d) > \varepsilon_*(k_2, d) > \varepsilon_*(k_3, d) > \dots, \text{ for } d > d_k.$$

- (3) *Define $d_{0,1} = +\infty$, and as k increases, $d_M(k)$ decreases monotonically. Therefore, when $k = 0$, $d_M(0)$ is the largest.*

- (4) *Define*

$$\varepsilon_* = \varepsilon_*(d) = \varepsilon_*(k, d), k \in (d_{k_{i+1}, i+2}, k_{i, i+1}), k_i \in N, i = 1, 2, 3, \dots,$$

then

$$\varepsilon_*(d) \leq \varepsilon_B(d), 0 < d < +\infty.$$

Moreover, $\varepsilon_*(d) = \varepsilon_B(d)$, if and only if $d = d_M(k)$, $k \in N$.

Proof. (i) When $d = d_M(k)$, $\varepsilon_*(d)$ takes the maximum value ε_1 . That is, $\varepsilon_*(d) = \varepsilon_1$. Therefore, $\varepsilon_*(d) \leq \varepsilon_1$.
(ii) $\varepsilon_*(d) = \varepsilon_*(k, d) = \frac{l^2[p_1 dk^2 \pi^2 - p_1 p_2 l^2 - q_1 q_2 l^2]}{dk^2 \pi^2 (dk^2 \pi^2 - p_2 l^2)} < \frac{l^2 p_1 dk^2 \pi^2}{dk^2 \pi^2 (dk^2 \pi^2 - p_2 l^2)} < \frac{p_1 l^2}{d \pi^2 - p_2 l^2} = \varepsilon_2(d)$. \square

In Figure 2, we characterize a graph of functions $\varepsilon = \varepsilon_1$, $\varepsilon = \varepsilon_2(d)$, and $\varepsilon = \varepsilon_*(k, d)$, $d > 0, k = 1, 2, 3, \dots$, which will help us understand the results of Lemma 2.2 and Lemma 2.3. In Figure 3, we present a graph of the Turing bifurcation line $\varepsilon = \varepsilon_*(d)$, $d > 0$.

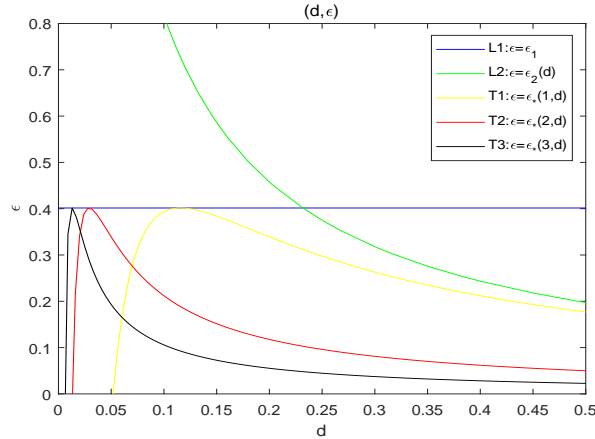


Figure 2. The figure of functions $\varepsilon = \varepsilon_1, \varepsilon = \varepsilon_2(d)$ and $\varepsilon = \varepsilon_*(k, d)$, $d > 0, k = 1, 2, 3$ in (d, ε) plane. Keeping the other parameters fixed at the values: $r = 4, m_C = 0.0201, K = 14.95, a_{CR} = 1.01, Th_{CR} = 1, ef_{RC} = 1, q_C = 0.05$.

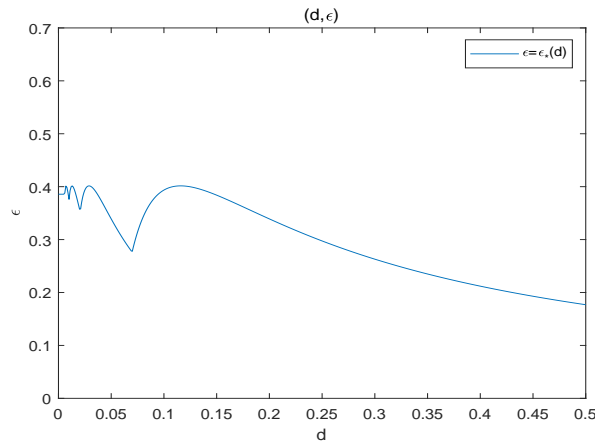


Figure 3. The Turing bifurcation line $\varepsilon = \varepsilon_*(d)$ ($d > 0$), while keeping the parameters fixed at the values: $r = 4, m_C = 0.0201, K = 14.95, a_{CR} = 1.01, Th_{CR} = 1, ef_{RC} = 1, q_C = 0.05$.

Theorem 2.2. Suppose that (B_0) holds.

- (1) For any given $k_1 \in \mathbb{N}$, when $\varepsilon = \varepsilon_*(k_1, d)$, system (2.5) occurs Turing bifurcation at (R_*, C_*) .
- (2) $\varepsilon = \varepsilon_*(d), d > 0$, is the critical curve of Turing instability.
- (i) If $\varepsilon > \varepsilon_*(d), d > 0$, system (2.5) is asymptotically stable at (R_*, C_*) .

(ii) If $0 < \varepsilon < \varepsilon_*(d)$, $d > 0$, Turing instability occurs in system (2.5) at (R_*, C_*) .

2.4. Existence of Hopf bifurcation

In this section, we mainly analyze the existence of Hopf bifurcation of the system (2.5). We assume that

$$(B'_0) \quad p_1 > \max\{-p_2, -\frac{q_1 q_2}{p_2}\}.$$

Denote

$$\varepsilon_H(k, d) = \frac{-dk^2\pi^2 + p_1 l^2 + p_2 l^2}{dk^2\pi^2}, 0 < d < d_k, \quad (2.9)$$

where $d_k = \frac{p_1 l^2 + p_2 l^2}{k^2 \pi^2}$, then $TR_k = 0$, when $\varepsilon = \varepsilon_H(k, d)$.

That is,

$$TR_k = 0 \Leftrightarrow \varepsilon_H(k, d) = \frac{-dk^2\pi^2 + p_1 l^2 + p_2 l^2}{dk^2\pi^2}.$$

Then, we can find $\varepsilon_H(k, d)$ decreases monotonically in d and intersects with $\varepsilon = \varepsilon_1$ at the point $d = d_H$, where

$$d_H = \frac{p_1 p_2^2 l^2 + p_2^3 l^2}{\pi^2 (k^2 p_1 p_2 + k^2 p_2^2 + 2k^2 q_1 q_2 - 2k^2 p_2^2 \sqrt{\frac{q_1 q_2 (p_1 p_2 + q_1 q_2)}{p_2^3}})}.$$

Theorem 2.3. Suppose that (B'_0) holds. For any given $k_1 \in N$, when $\varepsilon = \varepsilon_H(k_1, d)$, $0 < d < d_H$, system (2.5) occurs Hopf bifurcation at positive equilibrium (R_*, C_*) .

Proof. When $\varepsilon = \varepsilon_H(k_1, d)$, we have $TR_{k_1} = 0$. Then, (2.6) becomes

$$\lambda^2 + DET_{k_1} = 0. \quad (2.10)$$

Since $\varepsilon_H(k_1, d) > \varepsilon_1$, through assumption (B'_0) , $DET_{k_1} > 0$, we know that (2.10) has a pair of pure imaginary roots. The above satisfies conditions for the generation of Hopf bifurcation. \square

3. Numerical simulations

3.1. Numerical simulations of Turing bifurcation

Let $D_R = 0.03$, $D_C = 0.41$, $m_C = 0.722$, $r = 0.61$, $K = 14.95$, $a_{CR} = 1.01$, $Th_{CR} = 1$, $ef_{RC} = 1$, $q_C = 0.05$, $l = 1$, $k = 1$, we obtain positive equilibrium of system (2.5) is $(R_*, C_*) = (5.48169, 2.50026)$, and $p_1 = 0.103561$, $p_2 = -0.125013$, $q_1 = 0.847013$, $q_2 = 0.0591038$. Through (B_1) , (B_2) , equations (2.7) and (2.8), we obtain $\varepsilon_1 = 0.0618551$,

$$\varepsilon_B(d) = \begin{cases} 0.0618551, & 0 < d \leq 0.156971, \\ \frac{0.103561}{d\pi^2 + 0.125013}, & d > 0.156971, \end{cases}$$

and

$$\varepsilon_*(k, d) = \frac{0.103561 dk^2 \pi^2 - 0.0371152}{dk^2 \pi^2 (dk^2 \pi^2 + 0.125013)}.$$

Then, we can find $\varepsilon > \varepsilon_*(d)$, so the system (2.5) is asymptotically stable at (R_*, C_*) . The following Figure 4 shows that the system (2.5) is asymptotically stable at the positive equilibrium point (5.48169, 2.50026).

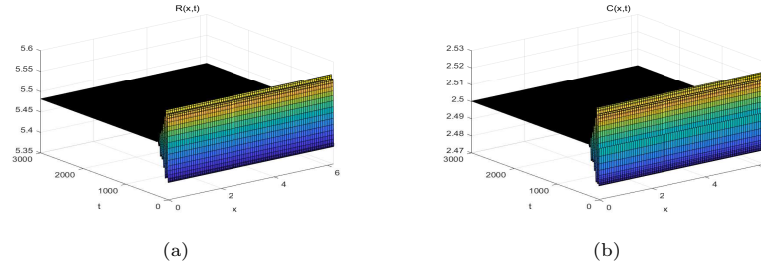


Figure 4. The numerical simulations of system (2.5) with $\varepsilon = 0.0732$ and the initial condition at (5.4, 2.5). (a): component R (Locally asymptotically stable); (b): component C (Locally asymptotically stable).

Let $D_R = 0.01, D_C = 0.3, m_C = 0.722, r = 0.61, K = 14.95, a_{CR} = 1.01, Th_{CR} = 1, e_{f_{RC}} = 1, q_C = 0.05, l = 1$, we obtain positive equilibrium of system (2.5) is $(R_*, C_*) = (5.48169, 2.50026)$, and $p_1 = 0.103561, p_2 = -0.125013, q_1 = 0.847013, q_2 = 0.0591038$. Through $(B_1), (B_2)$, equations (2.7) and (2.8), we obtain $\varepsilon_1 = 0.0618551$,

$$\varepsilon_B(d) = \begin{cases} 0.0618551, & 0 < d \leq 0.156971, \\ \frac{0.103561}{d\pi^2 + 0.125013}, & d > 0.156971, \end{cases}$$

and

$$\varepsilon_*(k, d) = \frac{0.103561dk^2\pi^2 - 0.0371152}{dk^2\pi^2(dk^2\pi^2 + 0.125013)}.$$

By setting $k = 1$, we obtain $d_{0,1} = +\infty$ and $d_{1,2} = 0.0477964$. Select $d = d_1 = 0.05 \in (d_{1,2}, d_{0,1})$, thus $\varepsilon_* = \varepsilon_*(1, 0.05) = 0.0416967$. Equation (2.5) with $d = 0.05$ undergoes Turing bifurcation near equilibrium (5.48169, 2.50026) at $\varepsilon = 0.0416967$. Figure 5 shows that the system (2.5) has Turing instability near the equilibrium point (5.48169, 2.50026) at this time.

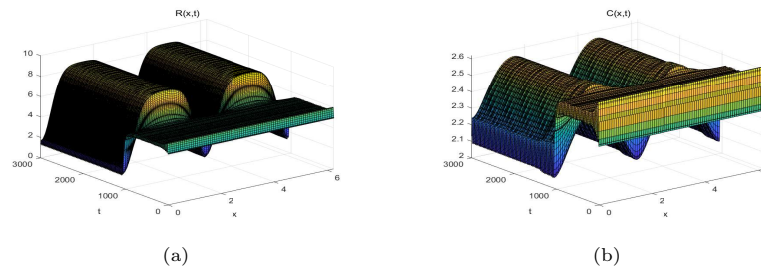


Figure 5. The numerical simulations of system (2.5) with $\varepsilon = 0.033$ and the initial condition at (5, 2.5). (a): component R (Turning instability); (b): component C (Turning instability).

3.2. Numerical simulations of Hydra effect

At this point, we can find that when the mortality rate of predator C is reduced, the population size of this population also decreases. This is consistent with the phenomenon of hydra effect mentioned in Lucas dos Anjos's article [3]. The following Figure 6 shows the changes in the population of predator C , when the mortality rate of predator C is equal to 0.722 and 0.717 respectively. The existence of the hydra effect is proved, when the system has a non-homogeneous steady-state solution.

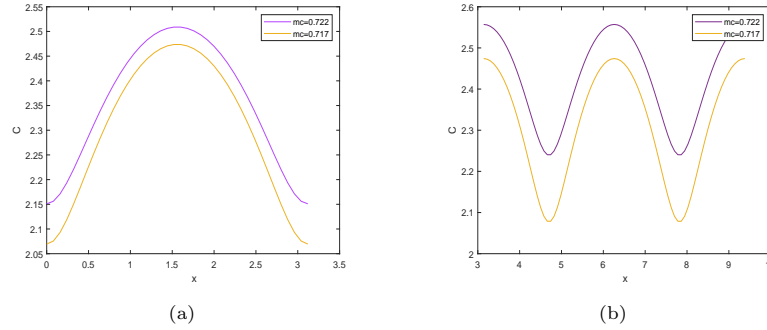


Figure 6. Spatial distribution of predator resulting from model simulations response for two values of the per capita mortality rate of the predator ($mc=0.722$ and $mc=0.717$), while keeping the parameters fixed at the values: $D_R = 0.01$, $D_C = 0.3$, $r = 0.61$, $K = 14.95$, $a_{CR} = 1.01$, $Th_{CR} = 1$, $ef_{RC} = 1$, $q_C = 0.05$, $l = 1$. $x \in (0, \pi)$ and $x \in (\pi, 3\pi)$ in (a) and (b) respectively.

3.3. Numerical simulations of Hopf bifurcation

Let $D_R = 0.91$, $D_C = 0.81$, $m_C = 0.51$, $r = 0.81$, $K = 14.95$, $a_{CR} = 1.01$, $Th_{CR} = 1$, $ef_{RC} = 1$, $q_C = 0.05$, $l = 10$, we obtain positive equilibrium of system (2.5) is $(R_*, C_*) = (1.48734, 1.80708)$. Then, we obtain $p_1 = 0.357322$, $p_2 = -0.0903541$, $q_1 = 0.600354$, $q_2 = 0.291508$. Through assumption (B_1) and (2.9), we have $\varepsilon_1 = 0.201445$ and

$$\varepsilon = \varepsilon_H(k, d) = \frac{-dk^2\pi^2 + 26.6968}{dk^2\pi^2}.$$

We can obtain $d_H = 0.204694$. We choose $d = 0.2$, which is satisfied $d < d_H$, and obtain $\varepsilon_H = 12.5248$. The relationship between $\varepsilon = \varepsilon_1$ and $\varepsilon = \varepsilon_H(k, d)$ can be reflected by Figure 7. The following Figure 8 shows the numerical simulations of system (2.5) with Hopf bifurcation.

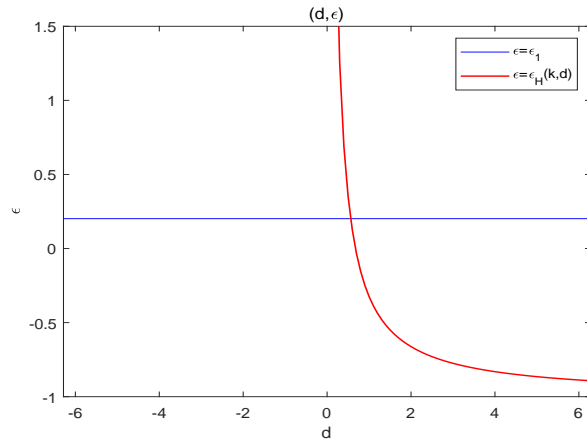


Figure 7. The figure of functions $\varepsilon = \varepsilon_1$, and $\varepsilon = \varepsilon_H(k, d)$ in (d, ε) plane

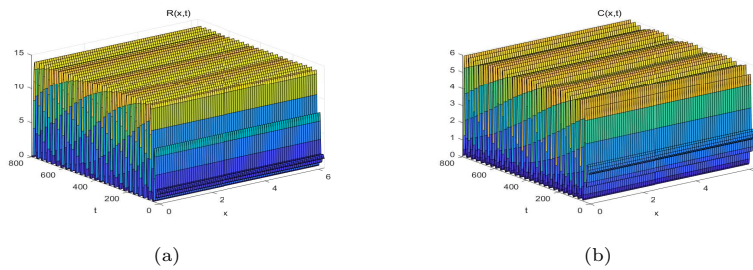


Figure 8. The numerical simulations of system (2.5) with $\varepsilon = 1.1235$ and the initial condition at (1.4, 1.8). (a): component R (Hopf bifurcation); (b): component C (Hopf bifurcation).

Moreover, we observe that $R(x, t)$ and $C(x, t)$ are periodic in relation to t . That is, there is a stable bifurcation periodic solution near the positive equilibrium of equation (2.5). In order to understand this sentence better, we have drawn the projection curves of the three-dimensional figures of the Hopf bifurcation on the $t - R$ and $t - C$ planes in Figure 9.

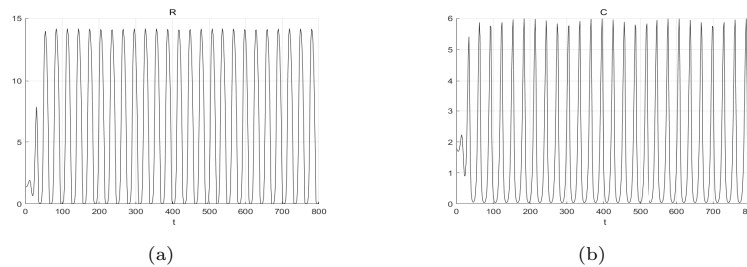


Figure 9. (a) and (b) describe the $R(x, t)$ and $C(x, t)$ periodic solution images respectively.

4. Conclusion

The system (1.1) is a reaction diffusion predator-prey model with a functional response function $F(R)$. This paper studies the influence of diffusion coefficient on the number of populations on the original basis. Meanwhile, a combination of theoretical analysis and numerical simulation is used to verify the existence of the hydra effect. It is concluded that as the diffusion coefficient changes, the population size may become no longer stable, or it may change periodically around the equilibrium amount. In practical applications, we can adjust the parameters according to specific goals, and then achieve the best results combined with reality. From a biological point of view, we explain the existence of the hydra effect, when Turing instability occurs in the system.

Acknowledgements

The authors would like to thank the editors and reviewers for their helpful comments.

References

- [1] P. A. Abrams, *When does greater mortality increase population size? The long history and diverse mechanisms underlying the hydra effect*, Ecology Letters, 2009, 12(5), 462–474.
- [2] P. A. Abrams and H. Matsuda, *The effect of adaptive change in the prey on the dynamics of an exploited predator population*, Canadian Journal of Fisheries and Aquatic Sciences, 2005, 62(4), 758–766.
- [3] L. dos Anjos, M. I. da S. Costa and R. C. Almeida, *Characterizing the existence of hydra effect in spatial predator–prey models and the influence of functional response types and species dispersal*, Ecological Modelling, 2020, 428, Article ID 109109, 9 pages.
- [4] X. Cao and W. Jiang, *Turing–Hopf bifurcation and spatiotemporal patterns in a diffusive predator–prey system with Crowley–Martin functional response*, Nonlinear Analysis: Real World Applications, 2018, 43, 428–450.
- [5] R. Dager, V. Navarro and M. Negreanu, *Uniform boundedness for a predator–prey system with chemotaxis and dormancy of predators*, Quarterly of Applied Mathematics, 2021, 79(2), 367–382.
- [6] B. Dubey, Sajjan and A. Kumar, *Stability switching and chaos in a multiple delayed prey–predator model with fear effect and anti-predator behavior*, Mathematics and Computers in Simulation, 2021, 188, 164–192.
- [7] M. E. M. Hacini, D. Hammoudi and S. Djilali, *Optimal harvesting and stability of a predator–prey model for fish populations with schooling behavior*, Theory in Biosciences, 2021, 140(2), 225–239.
- [8] W. Jiang, H. Wang and X. Cao, *Turing instability and Turing–Hopf bifurcation in diffusive schnakenberg systems with gene expression time delay*, Journal of Dynamics and Differential Equations, 2019, 31(4), 2223–2247.

- [9] S. Li and S. Guo, *Permanence of a stochastic prey–predator model with a general functional response*, Mathematics and Computers in Simulation, 2021, 187, 308–336.
- [10] Z. Liu and R. Yang, *Hopf Bifurcation Analysis of a Host–generalist Parasitoid Model with Diffusion Term and Time Delay*, Journal of Nonlinear Modeling and Analysis, 2021, 3(3), 447–463.
- [11] D. Luo and Q. Wang, *Dynamic analysis on an almost periodic predator–prey system with impulsive effects and time delays*, Discrete and Continuous Dynamical Systems. Series B., 2021, 26(6), 3427–3453.
- [12] K. M. McIntire and S. A. Juliano, *How can mortality increase population size? A test of two mechanistic hypotheses*, Ecology, 2018, 99(7), 1660–1670.
- [13] R. Ma, S. Li and S. Guo, *Steady–state solution for reaction–diffusion models with mixed boundary conditions*, Journal of Nonlinear Modeling and Analysis, 2019, 1(4), 545–560.
- [14] M. Qu, C. Zhang and X. Wang, *Analysis of dynamic properties on forest restoration–population pressure model*, Mathematical Biosciences and Engineering, 2020, 17(4), 3567–3581.
- [15] A. Sharma, A. K. Sharma and K. Agnihotri, *Analysis of a toxin producing phytoplankton–zooplankton interaction with Holling IV type scheme and time delay*, Nonlinear Dynamics, 2015, 81(1–2), 13–25.
- [16] M. Sieber and F. M. Hilker, *The hydra effect in predator–prey models*, Journal of Mathematical Biology, 2012, 64(1–2), 341–360.
- [17] C. M. Strevens and M. B. Bonsall, *The impact of alternative harvesting strategies in a resource–consumer metapopulation*, Journal of Applied Ecology, 2011, 48(1), 102–111.
- [18] X. Tang and Y. Song, *Stability, Hopf bifurcations and spatial patterns in a delayed diffusive predator–prey model with herd behavior*, Applied Mathematics and Computation, 2015, 254, 375–391.
- [19] J. Wang, J. Shi and J. Wei, *Dynamics and pattern formation in a diffusive predator–prey system with strong Allee effect in prey*, Journal of Differential Equations, 2011, 251(4–5), 1276–1304.
- [20] Y. Wang, G. Lin and Y. Niu, *Travelling wave solutions in a predator–prey integrodifference system*, Journal of Difference Equations and Applications, 2021, 27(4), 512–530.
- [21] X. Yan and C. Zhang, *Stability and Turing instability in a diffusive predator–prey system with Beddington–DeAngelis functional response*, Nonlinear Analysis: Real World Applications, 2014, 20, 1–13.
- [22] R. Yang and C. Zhang, *The effect of prey refuge and time delay on a diffusive predator–prey system with hyperbolic mortality*, Complexity, 2016, 50(3), 105–113.
- [23] F. Yi, J. Wei and J. Shi, *Bifurcation and spatiotemporal patterns in a homogeneous diffusive predator–prey system*, Journal of Differential Equations, 2009, 246(5), 1944–1977.

-
- [24] C. Zhang, B. Zheng and P. Yu, *Second-order Normal Forms for n -dimensional Systems with a Nilpotent Point*, *Journal of Applied Analysis and Computation*, 2020, 10(5), 2233–2262.